Werk

Jahr: 1986
Kollektion: fid.geo
Signatur: 8 Z NAT 2148:59
Digitalisiert: Niedersächsische Staats- und Universitätsbibliothek Göttingen
Werk Id: PPN1015067948_0059
PURL: http://resolver.sub.uni-goettingen.de/purl?PPN1015067948_0059

LOG Id: LOG_0045
LOG Titel: Deconvolution as a method for the separation of Pi2 pulsations from background field variations
LOG Typ: article

Übergeordnetes Werk

Werk Id: PPN1015067948
PURL: http://resolver.sub.uni-goettingen.de/purl?PPN1015067948
OPAC: http://opac.sub.uni-goettingen.de/DB=1/PPN?PPN=1015067948

Contact

Niedersächsische Staats- und Universitätsbibliothek Göttingen
Georg-August-Universität Göttingen
Platz der Göttinger Sieben 1
37073 Göttingen
Germany
Email: gdz@sub.uni-goettingen.de

J Geophys (1986) 59:195-201

Journal of Geophysics

Deconvolution as a method for the separation of Pi2 pulsations from background field variations

Jörg Behrens[1] **and Karl-Heinz Glaßmeier**[2]
Institut für Geophysik, Universität Münster, Corrensstr. 24, D-4400 Münster, Federal Republic of Germany

Abstract. In high-latitude magnetograms Pi2 pulsations are usually accompanied by pronounced background magnetic field variations due to substorm activity. A detailed analysis of Pi2 characteristics therefore requires a separation of the Pi2 signal from these background variations. The standard procedure to perform this separation is high-pass filtering. However, this is an insufficient way of separation as is discussed by means of artificial time series. An alternative procedure of separation is thus suggested which is based on the transient response theory of Pi2 pulsations. According to this theory a substorm magnetogram is regarded as the convolution of a driving function and a transfer function, where the latter is identified as the Pi2 pulsation. Subsequently, a model for the driving function is derived and a deconvolution filter designed. Application of this deconvolution filter to a large number of real substorm magnetograms shows that this filter may well be approximated by a second derivative filter. We suggest this filter is more useful in detrending high-latitude Pi2 records than using a simple high-pass filter.

Key words: Pi2 pulsations - Substorm onset - Transient response mechanism - Deconvolution

Introduction

Pi2 pulsations are transient magnetohydrodynamic waves associated with auroral brightenings or substorm onsets in the Earth's magnetosphere. Studying the properties of these transient waves not only helps in an understanding of hydromagnetic wave propagation in planetary magnetospheres, but also serves to elucidate in more detail the processes associated with X-type neutral line formation in the geomagnetic tail.

However, studying Pi2 signals is not an easy task as both Pi2 and substorm magnetic field variations are recorded simultaneously. At least, they are entities of one and the same physical process occurring in the Earth's magnetotail. It is therefore questionable whether the traditional treatment of high-latitude magnetograms as the addition of Pi2 pulsations and substorm magnetic field variations is justified at all, regarding a physical point of view. However, if one accepts that magnetic variations observed near substorm onset regions in high-latitudes are the sum of Pi2 pulsations, i.e. magnetic disturbances due to MHD waves, and substorm magnetic field variations due to the sudden enhancement of the westward polar electrojet, the following problem arises. As the rise time of the substorm onset magnetic signature, henceforth called background field variation, is typically about 2 min (e.g. Samson et al., 1985) and typical Pi2 periods are of the same order, simple high-pass filtering of magnetic field variations in the Pi2 period range results in a contamination of the Pi2 spectrum by parts of the background field spectrum (see also Stuart, 1972; Pashin et al., 1982).

To illustrate this problem Fig. 1 shows records of the D component of geomagnetic field variations observed at the three stations MAT, RIJ and NAM of the Scandinavian Magnetometer Array (SMA; see Küppers et al., 1979) on January 12, 1978, 2105-2130 UT, when a moderate substorm occurred in the geomagnetic tail. Data from the three stations NAM ($L \sim 4.5$), RIJ ($L \sim 5.5$) and MAT ($L \sim 6.5$) are chosen to represent records from mid-, subauroral- and high-latitude regions. In all three records the Pi2 pulsation, starting at about 2115 UT, is clearly identifiable. However, at MAT and RIJ the Pi2 magnetic signature appears together with pronounced background field variations, while at the mid-latitude station NAM hardly any trend in the record is visible.

Power spectra of the records shown are displayed in the bottom part of Fig. 1. For NAM a clear spectral peak at a frequency of 11 mHz appears, representing the Pi2 pulsation. Some indication of such a peak is still visible in the RIJ spectrum, but hardly detectable in the MAT record. It is this missing separation of the Pi2 spectrum and the background field spectrum which causes high-pass filtering to be an insufficient tool with which to study Pi2 pulsations, especially at high-latitudes.

To further demonstrate the shortcomings of a simple high-pass filtering procedure, artificial time series as shown in the upper part of Fig. 2 are regarded as H and D components of an observed geomagnetic varia-

1 *New address:* Dornier System GmbH, D-7990 Friedrichshafen, Federal Republic of Germany

2 *New address:* Institut für Geophysik und Meteorologie, Universität zu Köln, Albertus-Magnus-Platz, D-5000 Köln 41, Federal Republic of Germany

Offprint requests to: K.H. Glaßmeier

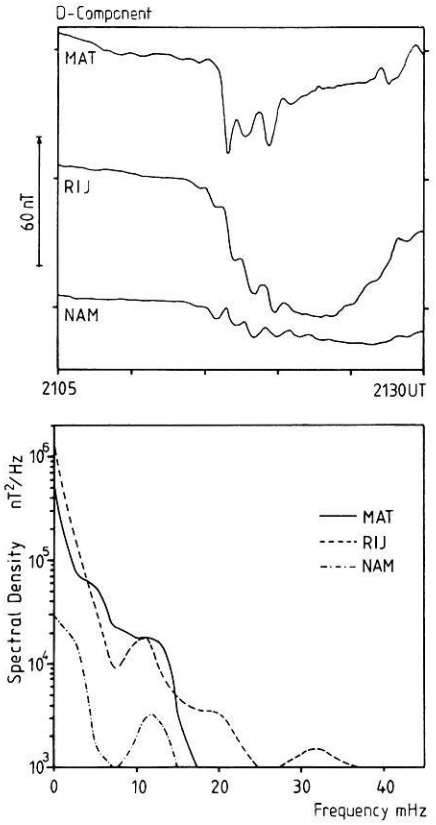

Fig. 1. *Upper panel:* substorm onset magnetograms recorded at three stations of the Scandinavian Magnetometer Array at different L values. *Lower panel:* power spectral density estimations of the corresponding time series

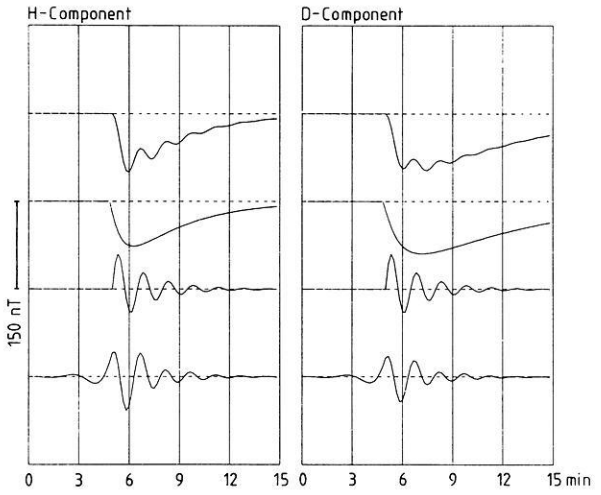

Fig. 2. Artificial magnetograms of horizontal H and D components *(upper traces)*. The following two panels show the used driving and transfer functions, respectively (see text). The corresponding high-pass filtered signals for each component are displayed in the lowest two panels

tion. Both artificial series result from a time convolution of the two functions $x(t)$ and $h(t)$ (the reason for using a convolution rather than the sum of $h(t)$ and $x(t)$ will be given later), where $x(t)$ is given by

$$x(t)=x_0 \exp(-\alpha t)\tan^{-1}(\beta t)$$

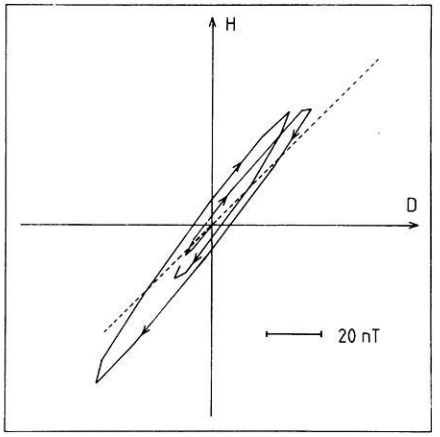

Fig. 3. Hodograms of the horizontal disturbance vectors of the Pi2 input *(dashed line)* and the high-pass filtered time series *(solid line)*, plotted for the first 450 s of the time series. For the latter hodogram, the sense of rotation is indicated by *arrows*

and regarded as the background field variation. $h(t)$ is regarded as an Pi2 signal and is given by

$$h(t)=h_0 \exp(-\gamma t)\sin(\delta t).$$

For the $H(D)$ component parameters $\alpha=5\times10^{-3}\,s^{-1}$ $(2.5\times10^{-3}\,s^{-1})$ and $\beta=2\times10^{-2}\,s^{-1}$ $(1.5\times10^{-2}\,s^{-1})$ have been chosen, while $x_0=-100$, $h_0=75$, $\gamma=8.3\times10^{-3}\,s^{-1}$ and $\delta=7\times10^{-2}\,s^{-1}$ are the same for both components. The background field variations, $x(t)$, and artificial Pi2 signals, $h(t)$, are displayed in the middle two traces of Fig. 2. Comparison of Figs. 1 and 2 also shows that the above parameter set results in sufficient similarity between observed magnetic variations during a substorm onset and the simulated ones.

Application of a standard high-pass filter (a Butterworth filter of order 8 is used) to the artificial H and D components results in the filtered signals shown in the bottom part of Fig. 2. Obvious differences between $h(t)$, the assumed Pi2 signal, and the filtered signals are given in the amplitude behaviour, where a distortion of the originally e-folding sinusoid oscillation may be seen. The sharp onset with the maximum amplitude at one quarter period of the input Pi2 is not reconstructed by the applied high-pass filter, with the consequence, that we now see the beginning of the oscillation shifted to earlier times.

It is not only the amplitude which is affected by the high-pass filter technique, but also the polarization of the two signals H and D. As can be seen from the above parameter set, H and D as constructed from $h(t)$ represent a linearly polarized signal, while after high-pass filtering of the simulated substorm magnetograms a clearly elliptically polarized Pi2 signal results as the hodogram in Fig. 3 shows.

As analysis of Pi2 polarization properties recently gave further important information on Pi2 generation mechanisms (e.g. Pashin et al., 1982, Samson and Harrold, 1983; Lester et al., 1984; Southwood and Hughes, 1985), our above comments demonstrate that a more refined method to separate the Pi2 signal from background field variation is necessary to reduce bias in amplitude and polarization studies of these pulsations.

Derivation of a deconvolution filter

In deriving the artificial H and D components displayed in Fig. 2 the time convolution between $x(t)$ and $h(t)$ rather than their sum has been used to construct an artificial substorm magnetogram. This is justified as current theories (e.g. Nishida, 1979; Kan et al., 1982; Baumjohann and Glaßmeier, 1984) regard Pi2 pulsations as the transient response of the magnetosphere-ionosphere system to sudden changes in the night-time magnetosphere.

Any change of, for example, the field-aligned current distribution in the magnetotail must be communicated to other parts of the magnetosphere by Alfvén waves. These Alfvén waves may bounce back and forth between conjugate ionospheres or other boundaries in the magnetosphere until a new current equilibrium is set up. For simple magnetospheric models, detailed expressions for the temporal and spatial variations of the magnetic and electric fields associated with such a transient Alfvén wave been given, e.g. by Lysak and Dum (1983) or Hughes (1983). In general, the temporal behaviour of such transients can be described as the convolution $y(t)$ of an impulse response $h(t)$ and a driving function $x(t)$

$$y(t)=\int_{-\infty}^{+\infty} h(\tau)\,x(t-\tau)\,d\tau=h(t)*x(t). \tag{1}$$

This approach is also in accord with early work by Boström (1972) who modelled the magnetosphere-ionosphere system by an equivalent current loop with lumped impedances, where Pi2 pulsations are excited by a 'switch-on' process of this current circuit.

Identifying $y(t)$ with measured magnetic variations, e.g. during a substorm event, it is natural to try to deconvolve the signal to get either information about the impulse response or the driving function. As both $x(t)$ and $h(t)$ are unknown, the deconvolution of $y(t)$ is a nonunique problem unless a sophisticated physical model for one of the functions is available. Because we regard Pi2 pulsations as transient responses of the magnetosphere-ionosphere system it seems natural to model the driving function and to reach the impulse response by a deconvolution of the measured signal. It is this impulse response function we regard as the desired Pi2 signal.

The driving function we like to identify as what we loosely call background field variation. A uniform definition of what is meant by background variation can not be given. However, it is a common feature of substorm magnetic signatures observed near the substorm onset region in high-latitudes that there is a sudden decrease of the magnetic field followed by a longer-lasting recovery phase. And it is this temporal trend which we regard as the driving function. As an empirical model for this temporal behaviour we assume an analytic function of the form

$$x(t)=\begin{cases}0 & t<0\\ c[\exp(-a\cdot t)-\exp(-b\cdot t)] & t>0\end{cases} \tag{2}$$

which closely resembles the characteristics of substorm-associated background field variations as displayed in Fig. 1. A large variability of the possible waveforms of the driving function is guaranteed by the three parameters a, b and c. For parameter values $a=1\times10^{-2}\,s^{-1}$, $b=2.5\times10^{-3}\,s^{-1}$ and an arbitrary value of c, the function $x(t)$ is displayed in Fig. 4. It is easily recognized that the chosen functional form $x(t)$ well reproduces typical features of the temporal behaviour of substorm magnetograms (as shown in Fig. 1), namely sudden decrease and longer-lasting recovery of the magnetic field.

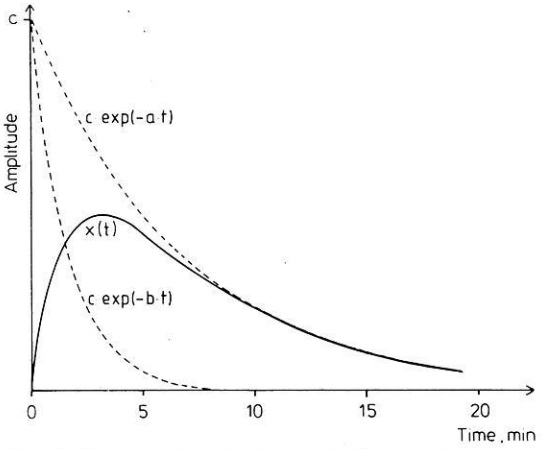

Fig. 4. Temporal variations of the functions $\exp(-at)$ and $\exp(-bt)$ as well as their compositions (see text)

It may well be argued that the choice of a functional form for $x(t)$ will seriously influence the measured $h(t)$. We are well aware of this problem, but a better choise requires a much more detailed understanding of the physical processes occurring in the Earth's magnetotail than presently available. Thus, our approach should be regarded as a first-order solution to a very complex problem.

A choice of a functional form $x(t)$ as given by Eq. (2) is also suitable for the following mathematical treatment as the deconvolution is best performed in the frequency domain. The z-transform of Eq. (2) is easily performed and for equidistant digital data with a sampling period Δt given by

$$X(z)=\frac{c(e^{-a\cdot\Delta t}-e^{-b\cdot\Delta t})\,z^{-1}}{(1-z^{-1}e^{-a\cdot\Delta t})(1-z^{-1}e^{-b\cdot\Delta t})} \tag{3}$$

from which the inverse operator

$$X^{-1}(z)=\frac{p}{z^{-1}}(1-gz^{-1}+fz^{-2}) \tag{4}$$

can be derived by taking the reciprocal, collecting terms and using the set of independent filter coefficients (p,f,g) instead of the set of independent parameters (c,a,b) with $g=e^{-a\cdot\Delta t}+e^{-b\cdot\Delta t}$, $f=e^{(-a-b)\cdot\Delta t}$, $p^{-1}=c(e^{-a\cdot\Delta t}-e^{b\cdot\Delta t})$, and $z=\exp(i\omega\Delta t)$. Note that due to our choice of $x(t)$ as given by Eq. (2), $X^{-1}(z)$ is a simple three-term and non-recursive phase-shift filter.

To find optimum coefficients p, f and g, a linear least-squares fit of the function $x(t)$ to the actually observed signal $y(t)$ is performed. The resulting parameter set a, b and c then gives the filter coefficients. As an example, Fig. 5 shows actually observed substorm magnetograms at stations EVE and MIK of the Scan-

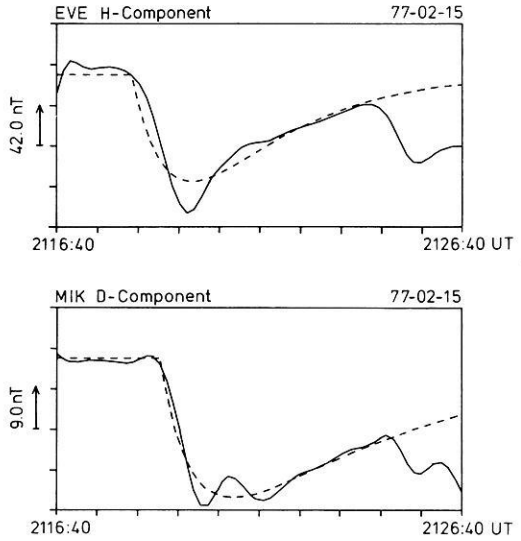

Fig. 5. Magnetograms of the H component recorded at station EVE and of the D component recorded at station MIK of the Scandinavian Magnetometer Array during the 77-02-15, 2118 UT substorm together with a linear least-squares fit *(dashed line)* of the function given by Eq. (2)

dinavian Magnetometer Array together with the fitted function $x(t)$. It can be seen that $x(t)$ describes the trend in the observed signals reasonably well.

However, working with magnetic field observations from an extended magnetometer array like the SMA (Küppers et al., 1979) the above-mentioned way to find the filter coefficients is inappropriate as the resulting coefficients for the different components at different locations are independently determined. Subsequent deconvolution of measured magnetic variations thus may violate physical constraints imposed on ground magnetic variations. Such a constraint, for example, is the irrotational character of the horizontal ground magnetic field (e.g. Fukushima, 1976; Glaßmeier, 1984). To conserve this property the filter coefficients can no longer be selected independently, but must fulfil certain conditions. However, to avoid an inter-component and inter-location dependent determination of the filter coefficients and to keep things as simple as possible, one may seek a uniform set of coefficients such that every signal is deconvolved by the same filter operator. Though this implies that each signal is no longer deconvolved in its optimum sense, the choice of a uniform set of filter coefficients guarantees to conserve, for example, the irrotational character of the ground magnetic field.

To determine such a uniform set of filter coefficients we analysed SMA data from two typical substorm events on February 15, 1977 (cf. Pashin et al., 1982) and January 12, 1978. For altogether 136 different horizontal and vertical components from 36 different stations the coefficients a, b and c have been determined by the linear least-squares procedure described above. With $\Delta t = 10$ s for the SMA data, the filter coefficients f and g (cf. Eq. 4) have been calculated and histograms of which are displayed in Fig. 6 together with the values of a and b. They show distributions with pronounced peaks at $a = 3 \times 10^{-3}\,\mathrm{s}^{-1}$, $b = 1.1 \times 10^{-2}\,\mathrm{s}^{-1}$, $f = 0.87$ and $g = 1.86$. Due to the small variance of the parameter distributions in Fig. 6 it is tempting to use the peak values of f and g as a uniform set of filter coefficients in our search for a filter operator (we keep the scaling factor p undetermined here for reasons to be discussed later):

$$X^{-1}(z) = \frac{p}{z^{-1}}(1 - 1.86z^{-1} + 0.87z^{-2}). \tag{5}$$

However, to justify the use of the above operator as a uniform filter it is advisable to study the properties of the filter operator as defined by Eq. (4) a little further. For this one can try to reduce the number of inde-

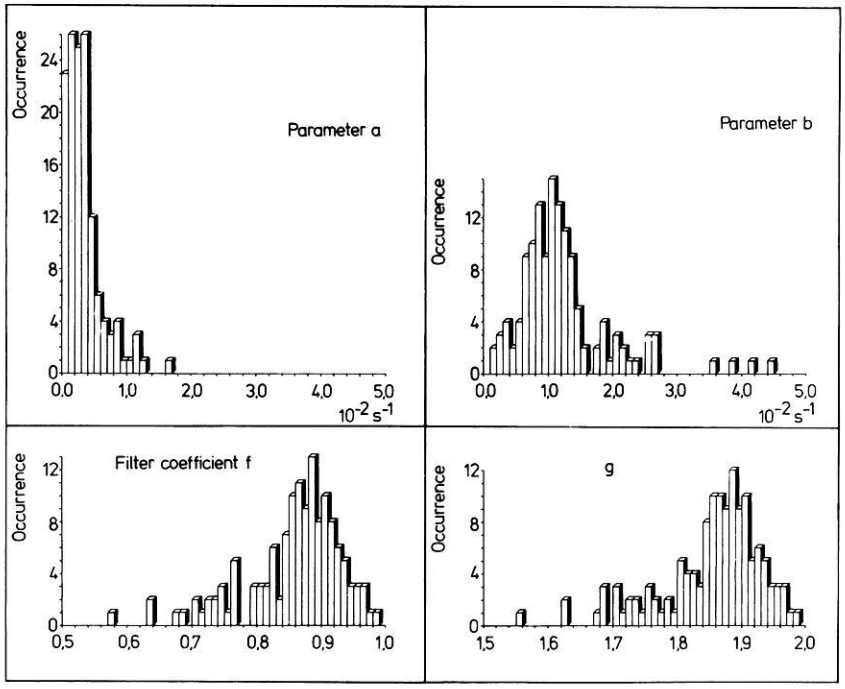

Fig. 6. Histograms of the parameters a and b as well as the corresponding filter coefficients f and g determined by fitting the analytic function $x(t)$ to real data by a linear least-squares fit (see text)

pendent variables in Eq. (4) and study the properties of the operator (4) as a function of one filter coefficient, either f or g. A relation between both is given by, for example,

$$g = e^{a \cdot \Delta t} f + e^{-a \cdot \Delta t} \tag{6}$$

which follows directly from their definition in Eq. (4). It should be noted that insertion of Eq. (6) in Eq. (4) does not reduce the number of independent variables in our filter operator. This is only accomplished after specifying a value for a.

With the peak value found for the parameter a, $3 \times 10^{-3}\,\mathrm{s}^{-1}$, and $\Delta t = 10$ s, Eq. (6) reduces to

$$g = 1.03 \cdot f + 0.97. \tag{7}$$

Insertion of this relation in Eq. (4) now leads to a filter operator which only depends on one parameter, f

$$X^{-1}(z) = \frac{p}{z^{-1}}\left[1 - (1.03f + 0.97)\, z^{-1} + f z^{-2}\right]. \tag{8}$$

The gain and phase responses of this filter are plotted in Fig. 7 for different values of the coefficient f in the interval $0 < f < 1$. It is obvious that changes of f do not affect the amplitude spectrum for larger values of f, i.e. the gain is relatively insensitive to variations of the parameter f. This holds especially for the values of f found from the analysis of the two substorm events (cf. Fig. 6), where f is always found to be larger than 0.6. From this it follows that our choice of the peak values of the f- and g-parameter distributions in Fig. 6 as a uniform set of filter coefficients still provides us with an optimum filter given by Eq. (5) as far as the gain response is concerned.

This does not apply to the phase response as Fig. 7 shows that small changes of f result in larger variations of the phase function. Thus a choice of the peak values of f and g as filter coefficients may no longer give us an optimum filter for a large class of signals as far as the phase response is concerned.

To tackle this dilemma we suggest using a zero-phase-shift filter. This certainly is a drawback from the idea of deconvolving substorm variations to yield the Pi2 waveform. However, one should keep in mind that both $x(t)$ and $h(t)$ in our deconvolution problem [cf. Eq. (1)] are undetermined, and that one has to look for a suitable model of $x(t)$. From the above discussion of the results displayed in Fig. 7 it is clear that the choice of a slightly incorrect model of $x(t)$ mainly affects the phase response rather than the gain. It is thus advisable to leave the phase spectrum of the signal to be analysed unchanged. In doing so one has to realize that one only yields an improvement of the amplitude - but not of the phase characteristics - of the Pi2 signal as compared with an ordinary high-pass filter. This still implies a contamination of the polarisation parameters of the Pi2 by phase information of the associated background field variations.

Using a filter operator like Eq. (8) a zero-phase-shift filter is realized by the choice $f = 1$ and $p < 0$, and the filter operator now reads

$$X^{-1}(z) = p(z^{+1} - 2 + z^{-1}). \tag{9}$$

The gain response of this filter is shown in Fig. 7 as a dashed line.

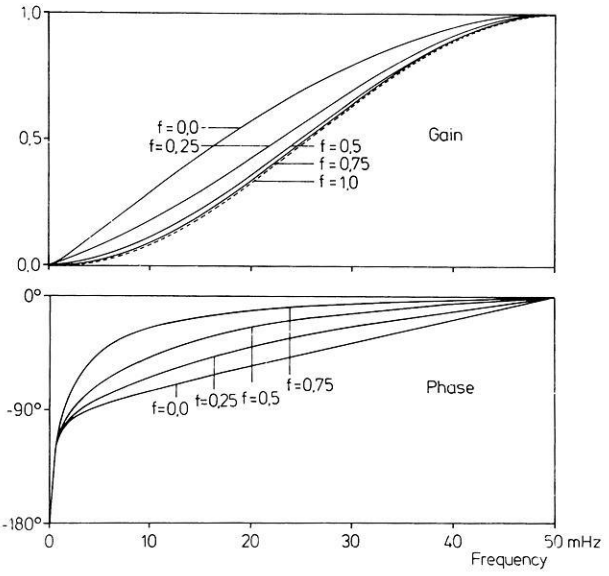

Fig. 7. Gain *(upper panel)* and phase *(lower panel)* characteristics of the deconvolution filter $X^{-1}(z)$ for different values of f

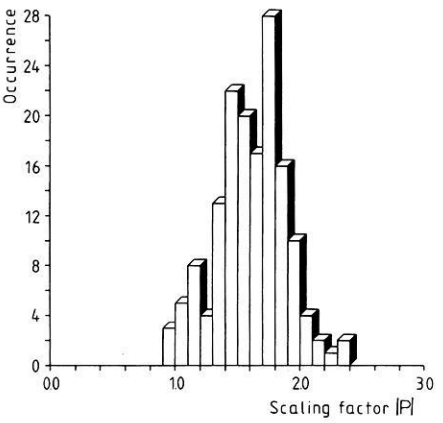

Fig. 8. Histogram of the modulus of the scale factor p determined by fitting the analytic function $x(t)$ to real data (see text)

As a multiplication by a factor z^{-1} means physically nothing but a delay of the time series by one sampling period, one may finally get the Pi2 time series $h(t)$ by

$$h_n = p(y_{n+1} - 2y_n + y_{n-1}) \tag{10}$$

where y_n denotes the n-th digital sample point of the input time series and h_n the corresponding one of the output series. Besides the scale factor p, $h(t)$ is nothing but the second derivative of the input time series.

Finally, the determination of the scale factor p remains. In principle one could follow a similar approach as for the filter coefficients f and g. A histogram for $|p|$ is given in Fig. 8. The distribution is as narrow as found before in the case of f and g (cf. Fig. 6). The peak value is $|p| = 1.7$. However, as this value represents the strength of an observed substorm event and is at least unpredictable, we suggest determining the scale factor p by normalizing the gain of $X^{-1}(z)$ to 1 at the supposed Pi2 frequency of a certain event rather than using some mean value of p.

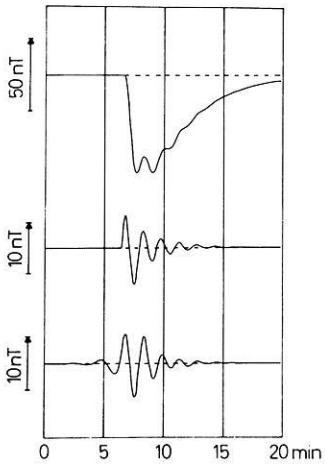

Fig. 9. Artificial substorm magnetogram *(upper trace)* and the corresponding deconvolution filtered time series *(middle trace)* as well as the high-pass filtered signal *(lower trace)*

Application aspects

To illustrate the efficiency, but also the weak points, of our approach to detrend Pi2 signals, in the following we want to discuss the analysis of artificial substorm magnetograms where the background field variations are not explicitly derivable from the analytical expression for $x(t)$ as used in Eq. (2) as well as a real magnetogram.

As a first example, Fig. 9 shows an artificial substorm onset magnetogram (upper time series) computed as the convolution between the driving function $x(t>0) = -100\tan^{-1}(9\times10^{-3}t)\exp(-5\times10^{-3}t)$ and the already used transfer function $h(t)$ (cf. Fig. 2). Use of the traditional high-pass filter (in our case a Butterworth filter of order 8 has been used) to separate Pi2 and substorm variations results in the time series shown as the bottom trace in Fig. 9. It has the already discussed defects, namely overshootings and oscillations before the true onset due to the Gibb's phenomenon. The deconvolution filter method suggested above, however, provides us with the time series displayed as the middle trace in Fig. 9. It suppresses the Gibb's phenomenon in an optimal way, provides us with a signal showing a very sharp onset and recovers, in a much better way than the high-pass filter, the highly damped waveform of the Pi2 pulsation which has initially been chosen as an e-fold damped sinusoid.

The improvement in recovering the Pi2 signal by using the deconvolution filter approach is also demonstrated by Fig. 10 where power spectra of the transfer function used in Fig. 9 (thick full line), the corresponding substorm magnetogram (thin full line), the standard filter magnetogram (dashed-dotted line) and the deconvolved time series (dotted line) are shown. The standard filtered magnetogram provides a spectrum which approximates that of the input Pi2 (thick full line) only roughly around its peak value at 11 mHz and at higher frequencies. However, the low-frequency part of the original spectrum is reproduced absolutely wrongly.

The deconvolution filtered magnetogram, on the other hand, provides a spectrum which approximates major portions of the original spectrum. Only the very-low-frequency part is less well reconstructed. Thus the

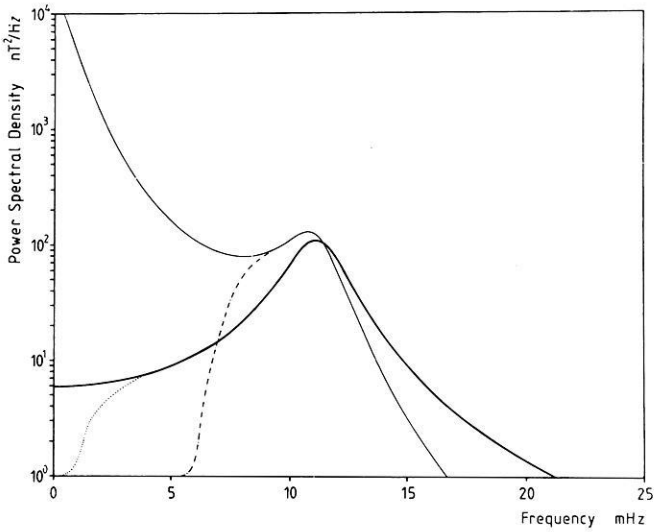

Fig. 10. Power spectral density estimates of the artificial substorm magnetogram *(thin full line)*, the high-pass *(dashed-dotted line)* and deconvolution filtered time series *(dotted line)* together with that of the original Pi2 signal *(thick full line)*

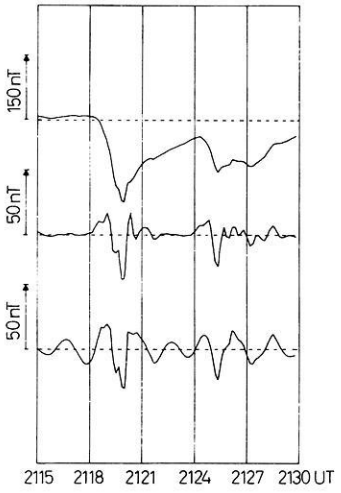

Fig. 11. High-latitude magnetogram *(upper trace)* with two successive substorm intensifications at 2118 and 2124 UT. The deconvolved time series *(middle trace)* shows the beginning of Pi2 pulsations with a clear separation of the two signals, whereas the standard high-pass filtered one *(lower trace)* is strongly superimposed by the oscillations of the filter response

deconvolution filter indeed represents a much better way to separate Pi2 and background magnetic variations.

An additional advantage of the deconvolution filter may be seen in Fig. 11 where a high-latitude substorm magnetogram showing two successive substorm onsets or intensifications is given. Using the standard high-pass magnetogram (lower panel) it is impossible to determine accurately either the first or the second onset time and therefore to separate both onsets and associated Pi2 trains. The deconvolution filter suggested, however, provides one with two clearly separated Pi2 signals (middle trace in Fig. 11). This may be useful to detect and distinguish in certain cases between several successive substorm intensifications, even when they are

separated from each other only by a short time interval.

Summary and conclusion

In the present paper we have discussed the shortcomings of using an ordinary high-pass filter to separate Pi2 pulsations from background field variations. It has been demonstrated that the Pi2 amplitude – as well as phase – characteristics are contaminated by background field variations in such a way that the interpretation of actually measured data may lead to wrong results.

In order to optimize the separation of the Pi2 signal from the background variations we propose a matched filter operator which is based on the 'transient response model' for Pi2 pulsations (cf. the review by Baumjohann and Glaßmeier, 1984). In this model a substorm magnetogram is regarded as resulting from a convolution of two time series, a driving function and a transfer function, where we interpret the latter as the Pi2 signal. As both driving and transfer functions are unknown for the Pi2 problem, we estimate the driving function to deconvolve substorm magnetograms. The deconvolution filter thus derived could be approximated by a three-term and zero-phase-shift filter.

The suggested filter operator may also be interpreted as a second-order difference filter and it is interesting to note that two-dimensional wavenumber second-derivative filters are commonly used to determine the trend or regional field and residual maps in gravity or magnetic data (e.g. Kulhánek, 1976, p. 148 and references therein). Thus our starting point, the transient response model for Pi2 pulsations (e.g. Nishida, 1979, Kan et al., 1982; Baumjohann and Glaßmeier, 1984), leads us to the same type of filter as also used to detrend data in other fields of geophysics.

Application of this filter to artificial magnetograms shows major advantages in recovering the Pi2 signals compared to an ordinary high-pass filter. The amplitude spectra of the filtered signals nearly coincide with the input Pi2 except at very low frequencies. An improvement of the phase spectrum, however, was not achieved due to our choice of a zero-phase-shift filter.

The performance of the deconvolution filter was also tested on a real high-latitude magnetogram, and it was demonstrated that the deconvolution filtered Pi2 signal has a much sharper onset than the usually filtered one. This property of the suggested filter might be of interest in further studies of Pi2 delay times across magnetometer arrays as recently done by Samson et al. (1985).

Concluding, we may say that at present an absolutely exact recovery of Pi2 signals, comprising the amplitude and the phase spectra, is impossible due to the lack of a sophisticated physical model of the driving function. However, under the given situation we were able to design a filter by using an empirical model, which requires a minimum number of parameters and which provides obviously better results as compared with those of standard high-pass filtering. We regard our new method in filtering Pi2s as a basis for constructing a more realistic filter for detrending these pulsations. Nevertheless, future work should be invested in a more detailed comparison between the polarization filter, introduced by Samson and Olson (1981), and the deconvolution filter, where perhaps a combination of these two different types of filters may provide improved Pi2 signals.

Acknowledgements. We would especially like to thank J. Untiedt for constant support and encouragement and W. Baumjohann, F. Glangeaud, G.K. Hartmann, R.L. McPherron and J.C. Samson for helpful discussions and constructive criticisms. Our work was financially supported by the Deutsche Forschungsgemeinschaft.

References

Baumjohann, W., Glaßmeier, K.H.: The transient response mechanism and Pi2 pulsations at substorm onset. Planet. Space Sci. **32**, 1361–1370, 1984

Boström, R.: Magnetospheric-ionospheric coupling. In: Critical problems of magnetospheric physics, E.R. Dyer, ed.: pp. 139–156. IUCSTP Secretariat, National Academy of Sciences, Washington D.C., 1972

Fukushima, N.: Generalized theorem of no ground magnetic effect of vertical current connected with Pedersen currents in the uniform conductivity ionosphere. Rep. Ionos. Space Res. Jpn. **30**, 35–40, 1976

Glaßmeier, K.H.: On the influence of ionospheres with non-uniform conductivity distribution on hydromagnetic waves. J. Geophys. **54**, 125–137, 1984

Hughes, W.J.: Hydromagnetic waves in the magnetosphere. In: Solar terrestrial physics, Carovillano, R.L., Forbes, J.M., eds. Dordrecht: D. Reidel Pub. Co., 1983

Kan, J.R., Longenecker, D.U., Olson, J.V.: A transient response model of Pi2 pulsations. J. Geophys. Res. **87**, 7483–7488, 1982

Kulhánek, O.: Introduction to digital filtering in geophysics. New York: Elsevier Scientific Publishing Company, 1976

Küppers, F., Untiedt, J., Baumjohann, W., Lange, K., Jones, A.G.: A two-dimensional magnetometer array for ground based observations of auroral zone electric currents during the International Magnetospheric Study (IMS). J. Geophys. **46**, 429–450, 1979

Lester, M., Hughes, W.J., Singer, H.J.: Longitudinal structure in Pi2 pulsations and the substorm current wedge. J. Geophys. Res. **89**, 5489–5494, 1984

Lysak, R.L., Dum, C.T.: Dynamics of magnetosphere-ionosphere coupling including turbulent transport. J. Geophys. Res. **88**, 365–380, 1983

Nishida, A.: Possible origin of transient dusk-to-dawn electric fields in the nightside magnetosphere. J. Geophys. Res. **84**, 3409–3412, 1979

Pashin, A.B., Glaßmeier, K.H., Baumjohann, W., Raspopov, O.M., Yahnin, A.G., Opgenoorth, H.J., Pellinen, R.J.: Pi2 magnetic pulsations, auroral break-ups, and the substorm current wedge: A case study. J. Geophys. **51**, 223–233, 1982

Samson, J.C., Olson, J.V.: Data adaptive polarization filters for multichannel geophysical data. Geophysics **46**, 1423–1431, 1981

Samson, J.C., Harrold, B.G.: Maps of the polarisation of high-latitude Pi2's. J. Geophys. Res. **88**, 5736–5744, 1983

Samson, J.C., Harrold, B.G., Yeung, K.L.: Characteristic time constants and velocities of mid-latitude Pi2's. J. Geophys. Res. **90**, 3448–3456, 1985

Southwood, D.J., Hughes, W.J.: Concerning the structure of Pi2 pulsations. J. Geophys. Res. **90**, 386–392, 1985

Stuart, W.F.: A special feature of impulsive pulsations (Pi2). J. Atmos. Terr. Phys. **34**, 829–836, 1972

Received September 16, 1985; revised version February 3, 1986
Accepted March 19, 1986